Global distributions and occurrence rates of transient luminous events

Alfred B. Chen,[1,2] Cheng-Ling Kuo,[1,8] Yi-Jen Lee,[1] Han-Tzong Su,[1,3] Rue-Ron Hsu,[1,3] Jyh-Long Chern,[4] Harald U. Frey,[5] Stephen B. Mende,[5] Yukihiro Takahashi,[6] Hiroshi Fukunishi,[6] Yeou-Shin Chang,[7] Tie-Yue Liu,[7] and Lou-Chuang Lee[8]

Received 16 February 2008; revised 24 March 2008; accepted 16 April 2008; published 15 August 2008.

[1] We report the global transient luminous event (TLE) distributions and rates based on the Imager of Sprites and Upper Atmospheric Lightning (ISUAL) experiment onboard the FORMOSAT-2 satellite. ISUAL observations cover 45°S to 25°N latitude during the northern summer and 25°S to 45°N latitude during the northern winter. From July 2004 to June 2007, ISUAL recorded 5,434 elves, 633 sprites, 657 halos, and 13 gigantic jets. Surprisingly, elve is the dominant type of TLEs, while sprites/halos are a distant second. Elve occurrence rate jumps as the sea surface temperature exceeds 26 degrees Celsius, manifesting an ocean-atmosphere-ionosphere coupling. In the ISUAL survey, elves concentrate over the Caribbean Sea, South China Sea, east Indian Ocean, central Pacific Ocean, west Atlantic Ocean, and southwest Pacific Ocean; while sprites congregate over central Africa, Japan Sea, and west Atlantic Ocean. The ISUAL experiment observed global rates of 3.23, 0.50, 0.39, and 0.01 events per minute for elves, sprites, halos, and gigantic jets, respectively. Taking the instrumental detection sensitivity and the restricted survey area into account, the corrected global occurrence rates for sprites and elves likely are a factor of two and an order of magnitude higher, respectively. ISUAL observations also indicate that the relative frequency of high peak current lightning (>80 kA) is 10 times higher over the oceans than over the land. On the basis of the corrected ISUAL elve global occurrence rate, the total electron content at the lower ionosphere above elve hot zones was computed to be elevated by more than 5%.

Citation: Chen, A. B., et al. (2008), Global distributions and occurrence rates of transient luminous events, *J. Geophys. Res.*, *113*, A08306, doi:10.1029/2008JA013101.

1. Introduction

[2] A serendipitous discovery in 1989 provided the first direct evidence for the existence of cloud-top flashes [*Franz et al.*, 1990], and opened up a research field to intensely study these phenomena now carrying the names of sprite [*Sentman et al.*, 1995; *Boeck et al.*, 1995; *Lyons et al.*, 1996; *Su et al.*, 2002; *Takahashi et al.*, 2003], elve [*Fukunishi et al.*, 1996; *Mende et al.*, 2005; *Frey et al.*, 2005], blue jet [*Wescott et al.*, 1995], halo [*Barrington-Leigh et al.*, 2001; *Moudry et al.*, 2003; *Miyasato et al.*, 2002], and gigantic jet [*Pasko et al.*, 2002; *Su et al.*, 2003; *van der Velde et al.*, 2007] (see Figure 1). A sprite consists of one or several vertical columns of light and spans the region between 40 and 90 km altitudes. A halo is a featureless luminous disk at 75–85 km altitudes, which may precede sprites but often also occurs alone. Both sprites and halos are associated with optical emissions caused by quasi-static electric fields produced by cloud-to-ground (CG) lightning [*Pasko et al.*, 1997], whereas elves are donut-shaped optical emissions in the ionosphere (altitude ~ 90 km) caused by the electromagnetic pulse (EMP) emitted by lightning strokes [*Inan et al.*, 1991; *Fukunishi et al.*, 1996]. Blue jets and gigantic jets are associated with upward electrical discharges from cloud tops. While the occurrence rate and global distribution of CG lightning in the troposphere has been extensively documented [*Christian et al.*, 2003; *Füllekrug and Constable*, 2000], those for TLEs are not well assessed because of limitations in previous space or ground observations. For example, *Sato and Fukunishi* [2003] deduced a global occurrence rate of 0.5 sprites/min (720 events per day) based on 216 days of ELF data containing ~715,500 transient Schumann resonance events. *Blanc et al.* [2004] inferred a global occurrence rate of 1.33 sprites/min from 3.5 hours of ISS observations. *Yair et al.* [2004] estimated the occurrence rate of 0.13 event/min for sprites using 13 orbits of video data of the STS-107 space shuttle mission (~51 minutes of

[1]Department of Physics, National Cheng Kung University, Tainan, Taiwan.
[2]Plasma and Space Science Center, National Cheng Kung University, Tainan, Taiwan.
[3]Earth Dynamical System Research Center, National Cheng Kung University, Tainan, Taiwan.
[4]Department of Photonics, National Chiao Tung University, Hsinchu, Taiwan.
[5]Space Sciences Laboratory, University of California, Berkeley, California, USA.
[6]Department of Geophysics, Tohoku University, Sendai, Japan.
[7]National Space Organization, HsinChu City, Hsinchu, Taiwan.
[8]Institute of Space Science, National Central University, Jhongli, Taiwan.

0148-0227/08/2008JA013101

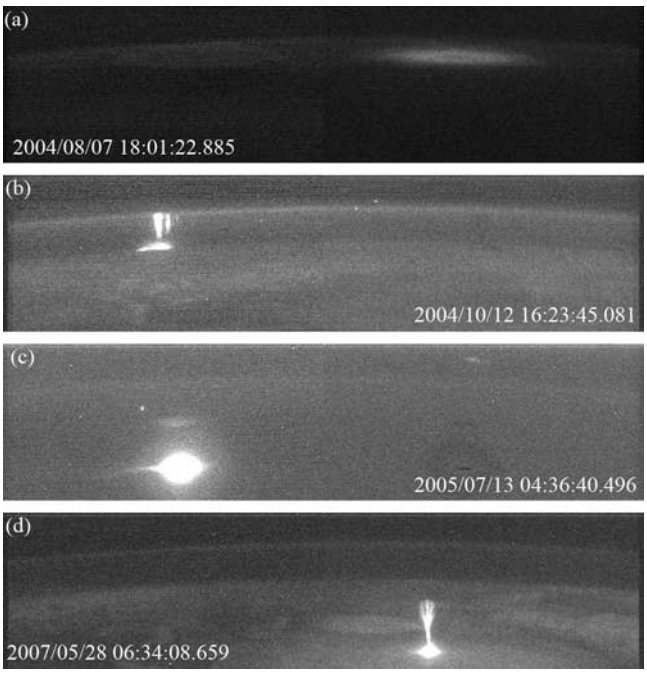

Figure 1. Representative ISUAL recorded TLE images: (a) elve, (b) sprite, (c) halo, and (d) gigantic jet.

thunderstorm footage). *Ignaccolo et al.* [2006] proposed a formula to give an estimated global sprite occurrence rate of 2.8 events/min based on optical observation data of less than 4 hours as well as 27 days of radio measurements. Here we report the global occurrence rates and distribution for the major types of TLEs based on three-year survey data from the ISUAL experiment. The instruments and observations are discussed in section 2, while the method of data analysis and statistical results are shown in section 3. In addition, we explore the dependence between the sea surface temperature and the occurrence rate of elves in section 5. Corrections to the observed occurrence rate and the global impact of elves are discussed in sections 6 and 7. Conclusions are presented in section 8.

2. Instrumentation and Observations

[3] The Imager of Sprites and Upper Atmospheric Lightning (ISUAL) [*Chern et al.*, 2003], the scientific payload onboard the FORMOSAT-2 satellite, is dedicated to a long-term and global survey of TLEs. ISUAL contains three bore-sighted sensors: an intensified CCD Imager, a six-channel spectrophotometer (SP) measuring photon fluxes at 6 pre-selected bands, and a 16-anode array photometer (AP) providing light variation at different vertical heights. The relevant specifications of these sensors are listed in Table 1. The FORMOSAT-2 spacecraft moves along a sun-synchronized orbit at 890 km altitude and ISUAL is configured with an eastward view observing TLEs over a region which is at a distance of 2,300 to 4,000 km away and close to local midnight. An ISUAL event was registered when the SP was triggered by either lightning or TLEs. The trigger levels were set empirically to optimize the detection of TLEs while keeping the false lightning events down; a constraint imposed on by the limited amount of the satellite onboard memory and data downlink bandwidth. For the northern summer, the ISUAL surveyed area roughly spans the region between 45°S and 25°N latitude; whereas for the northern winter, the ISUAL survey region covered 25°S to 45°N. The South Atlantic Anomaly region was excluded for the safety of the instruments. The known summer TLE hot zone of the US High Plains is also not included in this survey (see the third paragraph of section 4). The accumulative ISUAL observation time is displayed in Figure 2. The local time of the observed area ranges from 10:30 to 11:20 pm. Before ISUAL, only TLEs over a number of continental and costal areas were surveyed and studied from ground- and airborne-based platforms, because of the limitations of the local weather condition and geographical locations. Furthermore, atmospheric absorption also made investigations at the blue end of visible light and shorter wavelengths less favorable. Being the first long-term space survey, the ISUAL experiment has the potential to overcome the constraints associated with previous ground and aircraft observations. Indeed, ISUAL has conclusively confirmed the existence of FUV and MUV emissions in TLEs [*Mende et al.*, 2005; *Kuo et al.*, 2005, 2007].

3. Data Analysis

[4] The ISUAL recorded TLEs are categorized into sprites, halos, elves and gigantic jets based on their morphology in the imager (Figure 1) and with the assistance of light curves acquired by the SP and AP. The features of different types may be identified in one event simultaneously and be tallied respectively. The geographic coordinates of an ISUAL TLE are deduced from the imager frame with the assumption that the event or its parent thundercloud top were at certain heights [*Chen et al.*, 2005]: If the parent thundercloud is visible, we measure the position of the center or the brightest pixel of the illuminated cloud-top and take 15 km as the height of the thundercloud-top [*Smith et al.*, 1999], which is similar to the result of 14 km as reported by *Frey et al.* [2007]. If their parent clouds are not in sight, the top of sprites and the center of elves are assumed to be at 85 and 90 km high. The reading of event's image coordinates was done manually and a comparison among different individuals shows that the average variation is less than 2 pixels. To take this measurement error into account, a 2-D Gaussian "spatial distribution" was introduced. The final geographic location mapping on the Earth surface of an ISUAL event was achieved with the assistance of the associated time, instrument pointing, and position and attitude data of the FORMOSAT-2 spacecraft.

[5] The geolocation uncertainty of a TLE event, using the prescribed method, depends sensitively on the event distance and, on average, is better than 50 km/pixel along the line of sight. However, for events located above the Earth limb (distance to the spacecraft ~3,200 km), it can be as high as 220 km/pixel. Validations using the city light from major metropolitan areas show that our geolocating accuracy is better than 0.5° for objects within 2,800 km to the spacecraft [*Chen et al.*, 2004]. Fortunately, this geolocational error will not affect the assessment of the global TLE distribution.

4. Results

[6] From July 2004 to June 2007, more than 6,000 TLEs were recorded by ISUAL. The TLE event tally are listed in

Table 1. Relevant Specifications of the ISUAL Sensors

Instruments	Imager	SP	AP
Detector	intensified CCD with 524 × 128 pixels	six photomultiplier tubes	dual 16-anode arrays
Field of view	20° × 5°	20° × 5°	20° × 3.6°
Spatial resolution	0.04°/pixel	20° × 5°	0.23° per channel in vertical direction
Time resolution for the survey	programmable, 30 ms in this survey	0.1 ms	0.5 or 0.05 ms
Band passes	$N_2$1PG	three broadbands and three narrow bands	blue and red bands

Table 2, which shows the numbers of elves, sprites, halos, and gigantic jets observed as well as the percentage of each type occurring over the ocean, coast and land regions. Events containing more than one TLE type were tallied separately. The Earth surface is divided into 2.5° by 2.5° grids as was done by *Christian et al.* [2003]. We define the ocean and land grids as the earth surface regions that contain only ocean or land while the coast grids are those with a mixture of land and ocean areas. In the ISUAL survey region, 61% of total area is classified as ocean, 16% as coast, and 23% as land.

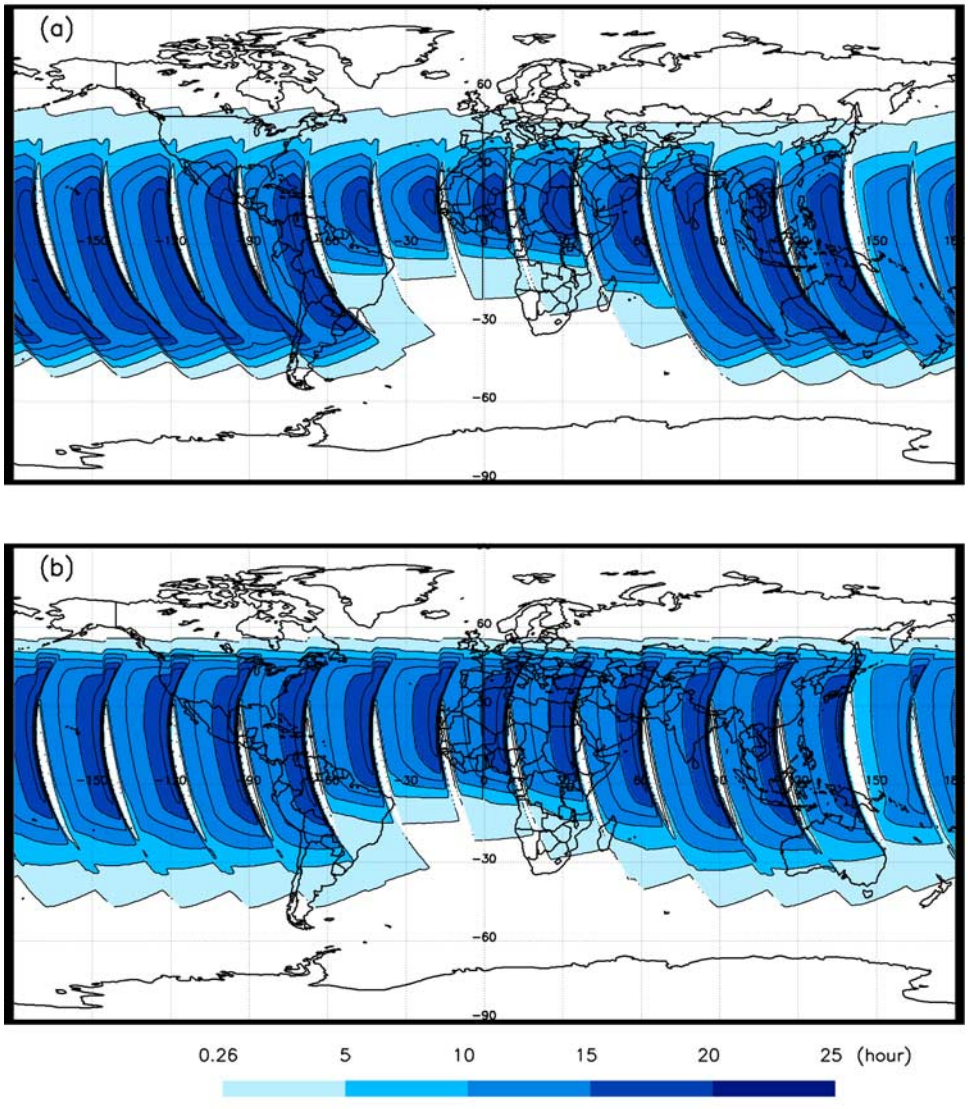

Figure 2. Accumulative observation time of ISUAL experiment between July 2004 and June 2007. (a) Northern summer (23 March–21 September). (b) Northern winter (22 September–22 March). Only the grid cells with sufficient accumulative observation time (higher than 30.7 minutes or 0.51 hours, see section 4) are denoted.

Table 2. Statistics of ISUAL TLE Survey for the Period from July 2004 to June 2007[a]

Type	Number	Land	Coast	Ocean	L:C:O (L&C:O) ratio
Elve	5434 (80.7%)	9%	32%	59%	0.4:2.1:1 (1.1:1)
Sprite	633 (9.4%)	49%	23%	28%	4.7:3.2:1 (4.1:1)
Halo	657 (9.8%)	21%	40%	39%	1.4:3.9:1 (2.4:1)
Gigantic jet	13 (0.2%)	15%	15%	69%	0.6:0.8:1 (0.7:1)

[a]The numbers of elves, sprites, halos and gigantic jets as well as the percentage of each type observed over ocean, coast, and land are tabulated. The last column is the ratio of occurrence per unit area over ocean (O), coast (C), and land (L).

[7] The occurrence density of each cell for a given type of TLE is defined as the cell accumulative event number (the sum of the spatial distributions) divided by the cell area and accumulative observation time. The ISUAL observed occurrence density distributions of sprites, elves and halos are shown in Figure 3 in the units of event/year/km^2. Figure 3d exhibits the distribution of mean sea surface temperature in the years 2004–2005 [*Vazquez et al.*, 1998] and it shows a tight correlation with the TLE occurrence density, which will be discussed later. The ISUAL observed TLE rate (r_{ISUAL}) is defined as the sum of TLE rates for the grid cells with a sufficient observation time, to avoid biased contributions from cells with a very low observation time. In this study, we choose 2.5% of the mean observation time of all observed grids during the three-year survey as the threshold for computing the occurrence rate, since the derived rates stabilize after the threshold for the observation time exceeds this value. Under this criterion, we considered only cells that were observed for at least 30.7 minutes in 3 years and the resulting cell area covered 81.02% of the Earth surface (Figure 2, shade-coded area). The r_{ISUAL} of elve, sprite, halo, and gigantic jet are derived to be 3.23, 0.50, 0.39, and 0.01 events per minute. Because of FORMOSAT-2's sun-synchronized orbit, the ISUAL derived occurrence rates are for the Earth at local time around midnight. *Füllekrug* [2004] reported that the hourly average occurrence of intense lightning at this local time is comparable to the diurnal mean. Therefore, the rates obtained by the ISUAL experiment likely are not biased by local time. Possible corrections to these values are discussed in section 6.

[8] During the northern hemisphere summer, the ISUAL payload has to be turned off before exiting the Earth's umbra around 25°N to protect the sensitive instruments from direct sunlight. Thus, the known TLE hot zones, like the U.S. High Plains [*Lyons et al.*, 1996; *Gerken et al.*, 2000] and the East China Sea [*Su et al.*, 2002], are not in the survey region, and vice versa for the south hemisphere during the northern winter.

[9] Gigantic jets were observed from space for the first time by ISUAL. During the 3-year survey, 13 gigantic jets

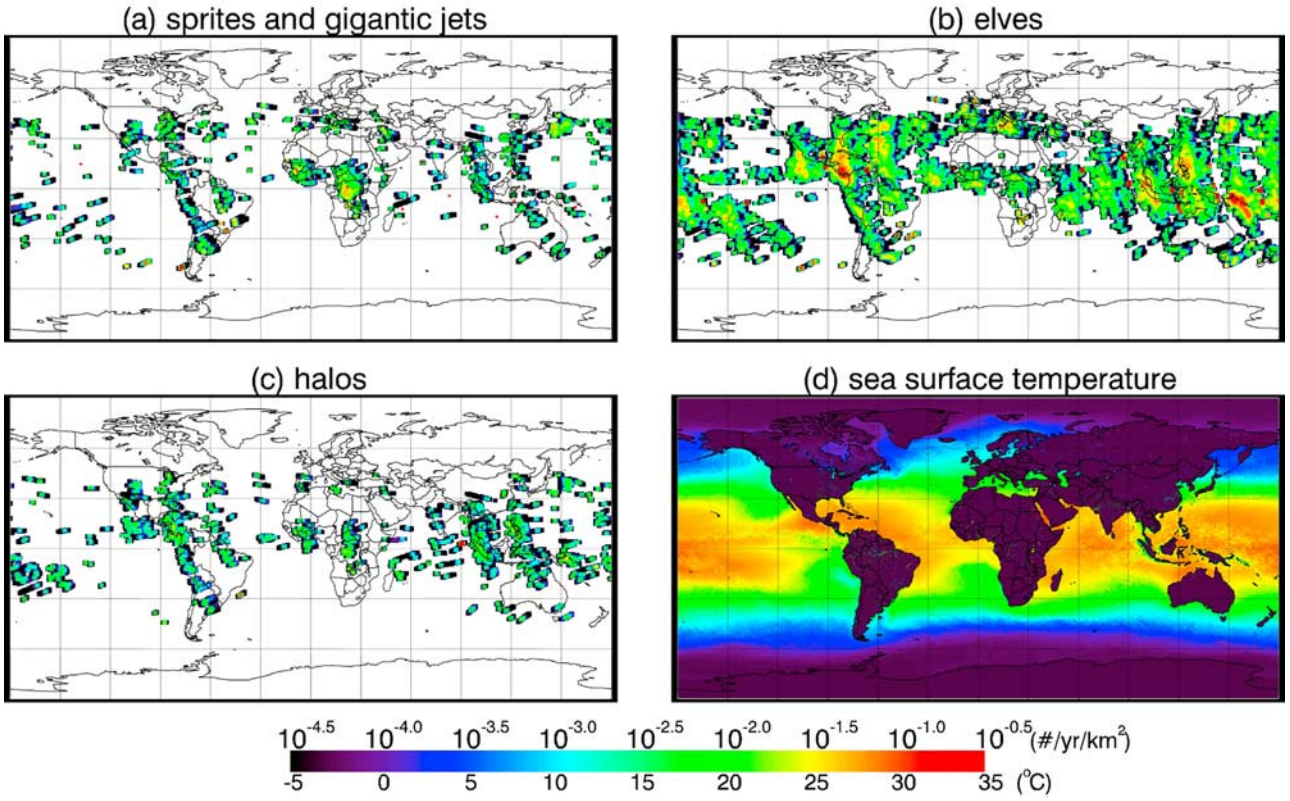

Figure 3. The global occurrence density of major TLEs: (a) sprites and gigantic jets (gigantic jets are marked by red filled circle), (b) elves, and (c) halos. The mean sea surface temperature between July 2004 and December 2005 is displayed in Figure 3d for comparison. (Data Source: PO.DAAC, JPL.)

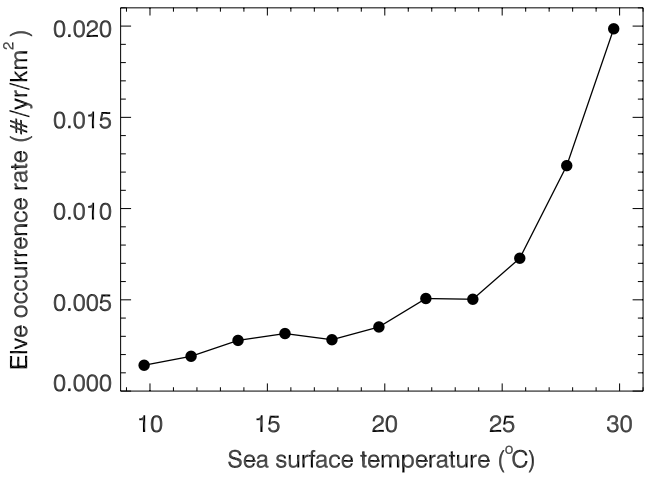

Figure 4. Elve occurrence rate versus sea surface temperature (SST). The elve occurrence rate increases rapidly when SST exceeds 26 degrees Celsius.

were recorded. Even though gigantic jets are observed rarely, the occurrence ratio between sprite and gigantic jet was found to be around 60. This ratio is comparable to the result from ground campaigns in the vicinity of Taiwan of ~80 (648 sprites and 8 gigantic jets in 6 years). These recorded gigantic jets were all located in the tropics, within 20° latitude of the equator.

[10] The land/coast-to-ocean ratio of CG lightning was reported to be 10:1 [*Christian et al.*, 2003], while the mean annual land(and coast)-to-ocean ratios for elve, sprite, and halo as shown in the last column (L&C:O) of Table 2 are 1.1:1, 4.1:1, and 2.4:1, respectively, after normalizing for the area. Obviously, elves concentrated over water with a significant percentage of 59% over the ocean but only 32% of elves over the coastal regions. Since elves are induced by the EMP from lightning strokes, the observed ratio is clearly discordant with that of the land-concentrated lightning flashes. On the other hand, sprites mainly congregate over land and coasts and have a comparable land (and coast)-to-ocean ratio as lightning. The land (and coast)-to-ocean ratio of halos fell between those of elves and sprites. It appears that the oceanic lightning strokes are much more effective in producing elves than their land counterpart. In the ISUAL surveyed area, the sprite hot zones are identified as Central Africa (Congo Basin), Japan Sea, and West Atlantic Ocean. In contrast, elves are found to be concentrated over Caribbean Sea, South China Sea, East Indian Ocean, Central Pacific Ocean, West Atlantic Ocean, and Southwest Pacific Ocean. For halos, the hot zones are similar to those for sprites, but with a lower land/coast-to-ocean ratio. No TLEs were found over desert areas (e.g., Sahara, Mongolia, and Central Australia deserts), and only a few were observed over the Northeast Pacific and Southeast Pacific Oceans.

5. Sea Surface Temperature and the TLE Occurrence Rates

[11] Since the tropical ocean is a good heat/energy reservoir in assisting vertical convection, we examine the relation between the elve occurrence rate and sea surface temperature (SST) as obtained from NODC/RSMAS AVHRR Oceans Pathfinder SST data [*Vazquez et al.*, 1998]. Figure 4 shows that the elve production rate depends strongly on SST. The elve occurrence rate increases rapidly when the SST exceeds 26 degrees Celsius. The threshold temperature of 26 degrees Celsius is also commonly accepted as a necessary condition for the development of a tropical storm, typhoon or hurricane [*Williams and Renno*, 1993]. A detailed examination of Figure 3 shows that the average surface temperature of some ocean areas with extremely low elve occurrence rates is lower than those in their vicinities. This finding provides direct evidence that the warm sea surface supplies the heat to produce the intense oceanic lightning responsible for elves. *Turman* [1977] showed that 11 of 17 recorded superbolts with optical power greater than 3×10^{12} watts were found over coast or ocean and concluded that oceanic lightning was more likely to produce superbolts. *Füllekrug et al.* [2002] compared the charge moment of CGs derived by ELF observations and arrived to a similar conclusion.

6. Corrected Global Occurrence Rate

[12] The brightness of elves is closely related to the power of the EMP emitted by the lightning return strokes, which in turn is linked to peak current. Figure 5 shows the model-computed correlation between the integrated photon flux of elves and the peak current of the return stroke (solid line). The theoretical elve photon flux is calculated using an EMP model [*Kuo et al.*, 2007] and the method is similar to the work of *Barrington-Leigh and Inan* [1999]. The detection limit of ISUAL is determined by the background fluctuation of the recorded images and typically is 1.5×10^3 photons/cm^2 (dotted line), which corresponds to an elve flux induced by a CG peak current of ~80 kA. The annual occurrence rate of negative CG lightning discharges recorded over North America by the National Lightning Detection Network (NLDN) from 1989 to 1995 [*Wacker and Orville*, 1999] is also plotted as a function of peak current. It can be seen that only ~0.82% of continental lightning events (red filled area) are able to trigger elves that are detectable by ISUAL. *Barrington-Leigh and Inan* reported that 52% of the NLDN flashes with peak current over 38 kA exhibited the telltale signature of elves, and above ~60 kA of peak current essentially all of the flashes had accompanying elves. About 6.3% of the NLDN flashes have a peak current greater than 60 kA (green- plus red-filled area), while lightning with peak current greater than 80 kA (red-filled area only) is almost eight times less likely. This implies that ~90% of elves are initiated by lightning with a peak current greater than 60 kA, but those from parent CG lightning with peak current of less than 80 kA could have been missed by ISUAL. Therefore the true global elve occurrence rate could be 10 times larger than that directly calculated from the ISUAL data and an estimated global occurrence rate of 35 elves per minute is derived.

[13] Close inspection of the SP light curves of the ISUAL registered columniform sprites shows that instrument recordings of these dimmer sprites were triggered by their parent lightning, not by the columniform sprites themselves. It is possible that some columniform sprites with their

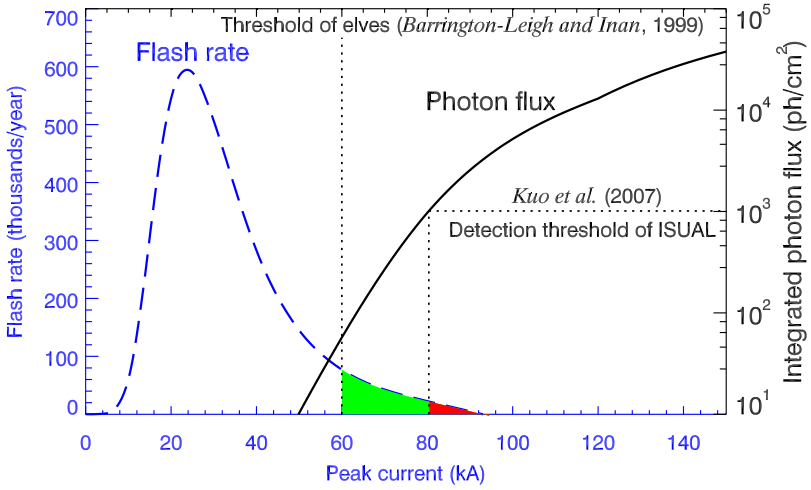

Figure 5. The model-computed correlation between the integrated photon flux of an elve and the peak current of the causative CG return stroke (solid line). The photon flux detection threshold of ISUAL is denoted by the dotted line, corresponding to a peak current of ~80 kA. The dashed line represents the annual occurrence rate of negative CG lightning discharges versus peak current over North America as recorded by NLDN from 1989 to 1995 [*Wacker and Orville*, 1999]. A threshold of 60 kA peak current reported by *Barrington-Leigh and Inan* [1999] is marked by the dotted line, and ~7% of lightning discharges (red and green area) are intensive enough to induce elves, but only less than 1% of continental negative CG lightning discharges (filled red area) can generate ISUAL detectable elves.

parent lightning outside the FOV, for example, behind the limb, might have been missed by ISUAL under the current trigger threshold. Also, note that known regions of high sprite occurrence, such as the U.S. High Plains in northern summer and parts of Brazil and Argentina in southern summer [*Thomas et al.*, 2007] are not viewed. It is difficult to estimate precisely how these two factors contribute to the underestimation of the global sprite occurrence rate. A factor of two higher is conjectured and it yields ~1 events/min for both sprites and halos. Thus, the global occurrence rate of all TLEs is ~40 events per minute, or 57,000 TLE events per day.

7. Global Impact of Elves

[14] In this paper, elves are identified as the dominant type of TLEs in the upper atmosphere. *Mende et al.* [2005], *Kuo et al.* [2007], and *Cheng et al.* [2007] demonstrated that elves manifest themselves not only in optical and UV emissions, but also in the increase of free electrons in the luminous region. With the global occurrence rate of elves obtained in the previous section, their contribution to the electron content of the ionospheric D-region can be assessed.

[15] The fractional global increase in total number of free electrons due to elves at the height of 80–90 km can be expressed as:

$$\mu = \frac{\Delta N_e}{N_e} = \frac{V_{elve} \cdot \Delta n_e \cdot r \cdot l}{V_{\oplus} \cdot n_e}, \tag{1}$$

where N_e and ΔN_e are the total number of ambient electrons and the change in the region of an elve. V_{elve}, $V_{\oplus}$, r, l are the volume of an elve, volume of the spherical shell between 80 and 90 km height, the global occurrence rate of elves and the lifetime of the free electrons at this height, respectively. In addition, n_e is the average electron density at the lower D-layer and Δn_e is the electron density change in an elve. We can also define the fractional increase of electron density in an elve as:

$$\alpha \equiv \frac{\Delta n_e}{n_e} \tag{2}$$

[16] Therefore, equation (1) can be rewritten as below:

$$\mu = \frac{V_{elve} \cdot \alpha \cdot r \cdot l}{V_{\oplus}} \tag{3}$$

[17] We assume elve has a cylindrical shape with a diameter D_{elve} of 165 km and vertically spans the height H between 80 km and 90 km, hence $V_{elve} = \pi(D_{elve}/2)^2 \times H$ [*Mende et al.*, 2005]. Here we adapt r as 35 events per minute as just discussed in the previous section. *Mika et al.* [2006] and *Cheng et al.* [2007] showed that the free electron clouds at the elve altitude can sustain for 2 minutes or more. Therefore, l is chosen as 2 minutes. *Rodger et al.* [2001] also noted that a strong lightning-EMP can lead to ~100% or even greater increase in the electron density at the lower ionosphere, hence $\alpha \geq 1$. *Mende et al.* [2005] demonstrated that an elve can produce an electron cloud with an average electron density of 210 cm^{-3} over a large circular region. On the basis of the IRI model [*Bilitza*, 2001], the mean night-times ambient electron density at 80–90 km is ~90 cm^{-3} and this leads to $\alpha \approx 1.3$. Hence we can safely take α to be unity. Plugging all of these values into equation (3), the average fraction of global electrons in the 80–90 km range produced by elves is $\mu \sim 1\%$.

[18] However, elves could exert a greater influence on the local electron density and chemical composition over the elve hot zones, since μ is proportional to the occurrence rate

r as shown in equation (3) and r has a geographical variation as large as an order of magnitude (see Figure 3b). We can rewrite equation (3) as below to emphasize the fractional local electron density change owing to elves:

$$\mu_{local} = \frac{V_{elve} \cdot \alpha \cdot r_{local} \cdot l}{V_{local}} \quad (4)$$

[19] Here V_{local} and r_{local} are the local volume of the spherical shell between 80 and 90 km height and the corresponding local occurrence rate of elves (after correction taken as described in the previous section). To demonstrate the local effect, we carry out the calculation for the Caribbean Sea hot zone (75–85°W and 5–15°N) using equation (4) and obtain $\mu_{local} \approx 5\%$ with $r_{local} \sim 1.5$ events/min. The 5% increase in the local electron density could have a significant impact on the local chemical equilibrium at the lower ionosphere. Hence, to model the atmospheric chemical reactions over the elve hot zones, a proper inclusion of the effect from elves may be required. Detailed assessment of the TLE contribution to the upper atmospheric energy budget and chemical composition will be presented in a separate paper.

8. Conclusions

[20] On the basis of a 3-year survey data from the ISUAL/FORMOSAT-2 experiment, 80% of recorded TLEs are elves, 20% are sprites or halos. The survey also yields the occurrence ratio between sprites and gigantic jets as ~60. Sprites mainly occur over land as lightning does, whereas elves occur mostly over oceans and coasts. The land/coast-to-ocean ratio of halos is between those of elves and sprites. A theoretical calculation based on a lightning peak current statistics indicates that only a very small fraction, less than 1%, of continental CG lightning are able to generate ISUAL detectable elves. We find, however, that the relative frequency of elves, and thus also of greater than 80 kA peak current lightning, is 10 times higher over ocean than over land. The strong dependence of elve occurrence over the sea surface temperature indicates that the warm tropical oceans provide the heat source to drive vertical convection and produce intense oceanic lightning, which in turn induce a large fraction of ISUAL recorded elves. This is a manifestation of ocean-atmosphere-ionosphere coupling. The increase of free electrons in the lower ionosphere from elves at global and local levels was also evaluated. Our results indicate that the global free electron contribution from elves is 1% approximately; however, the free electron content above elve hot zones could be elevated by more than 5%.

[21] **Acknowledgments.** This work was supported in part by the National Space Organization (NSPO) and the National Science Council in Taiwan under grants 97-NSPO(B)-ISUAL-FA09-01, NSC95-2111-M-006-002-MY2, and NSC96-2112-M-006-003-MY3. Thanks to S. A. Cummer, H. H. Hsu, and C. F. You for discussions, to S. F. Lin for operation supports, and to P. W. Kao, T. H. Huang, S. C. Wang, C. Y. Chiang, and C. T. Su for assistance.

[22] Zuyin Pu thanks Davis Sentman and another reviewer for their assistance in evaluating this paper.

References

Barrington-Leigh, C. P., and U. S. Inan (1999), Elves triggered by positive and negative lightning discharges, *Geophys. Res. Lett.*, *26*, 683–686.

Barrington-Leigh, C. P., U. S. Inan, and M. Stanley (2001), Identification of sprites and elves with intensified video and broadband array photometry, *J. Geophys. Res.*, *106*, 1741–1750.

Bilitza, D. (2001), International Reference Ionosphere 2000, *Radio Sci.*, *36*, 261–275.

Blanc, E., et al. (2004), Nadir observations of sprites from the International Space Station, *J. Geophys. Res.*, *109*, A02306, doi:10.1029/2003JA009972.

Boeck, W. L., et al. (1995), Observations of lightning in the stratosphere, *J. Geophys. Res.*, *100*, 1465–1475.

Chen, A. B., et al. (2004), ISUAL calibration and optimal ground coverage for detecting transient luminous events, *Eos Trans. AGU*, Fall Meet. Suppl., Abstract AE31B-0164.

Cheng, Z., S. A. Cummer, H.-T. Su, and R.-R. Hsu (2007), Broadband very low frequency measurement of D region ionospheric perturbations caused by lightning electromagnetic pulses, *J. Geophys. Res.*, *112*, A06318, doi:10.1029/2006JA011840.

Chern, J. L., et al. (2003), Global survey of upper atmospheric transient luminous events on the ROCSAT-2 satellite, *J. Atmos. Sol.-Terr. Phys.*, *65*, 647–659.

Chen, A. B., et al. (2005), Global distribution and seasonal distribution variation of transient luminous events, *Eos Trans. AGU Fall Meet. Suppl.*, Abstract AE23A-0991.

Christian, H. J., et al. (2003), Global frequency and distribution of lightning as observed from space by the Optical Transient Detector, *J. Geophys. Res.*, *108*(D1), 4005, doi:10.1029/2002JD002347.

Franz, R. C., R. J. Nemzek, and J. R. Winckler (1990), Television image of a large upward electrical discharge above a thunderstorm system, *Science*, *249*, 48–51.

Frey, H. U., et al. (2005), Beta-type stepped leader of elve-producing lightning, *Geophys. Res. Lett.*, *32*, L13824, doi:10.1029/2005GL023080.

Frey, H. U., et al. (2007), Halos generated by negative cloud-to-ground lightning, *Geophys. Res. Lett.*, *34*, L18801, doi:10.1029/2007GL030908.

Fukunishi, H., et al. (1996), Elves: Lightning-induced transient luminous events in the lower ionosphere, *Geophys. Res. Lett.*, *23*, 2157–2160.

Füllekrug, M. (2004), The contribution of intense lightning discharges to the global atmospheric electric circuit during April 1998, *J. Atmos. Sol.-Terr. Phys.*, *66*, 1115–1119.

Füllekrug, M., and S. Constable (2000), Global triangulation of intense lightning discharges, *Geophys. Res. Lett.*, *27*, 333–336.

Füllekrug, M., C. Price, Y. Yair, and E. R. Williams (2002), Intense oceanic lightning, *Ann. Geophys.*, *20*, 133–137.

Gerken, E. A., et al. (2000), Telescopic imaging of sprites, *Geophys. Res. Lett.*, *27*, 2637–2640.

Ignaccolo, M., et al. (2006), The planetary rate of sprite events, *Geophys. Res. Lett.*, *33*, L11808, doi:10.1029/2005GL025502.

Inan, U. S., et al. (1991), Heating and ionization of the lower ionosphere by lightning, *Geophys. Res. Lett.*, *18*, 705–708.

Kuo, C.-L., R. R. Hsu, A. B. Chen, H. T. Su, L. C. Lee, S. B. Mende, H. U. Frey, H. Fukunishi, and Y. Takahashi (2005), Electric fields and electron energies inferred from the ISUAL recorded sprites, *Geophys. Res. Lett.*, *32*, L19103, doi:10.1029/2005GL023389.

Kuo, C. L., et al. (2007), Modeling elves observed by FORMOSAT-2 satellite, *J. Geophys. Res.*, *112*, A11312, doi:10.1029/2007JA012407.

Lyons, W. A., et al. (1996), Sprite observations above the U.S. High Plains in relation to their parent thunderstorm systems, *J. Geophys. Res.*, *101*, 29,641–29,652.

Mende, S. B., et al. (2005), D region ionization by lightning-induced electromagnetic pulses, *J. Geophys. Res.*, *110*, A11312, doi:10.1029/2005JA011064.

Mika, Á., C. Haldoupis, T. Neubert, H. T. Su, R. R. Hsu, R. J. Steiner, and R. A. Marshall (2006), Early VLF perturbations observed in association with elves, *Ann. Geophys.*, *24*, 2179–2189.

Miyasato, R., M. J. Taylor, H. Fukunishi, and H. C. Stenbaek-Nielsen (2002), Statistical characteristics of sprite halo events using coincident photometric and imaging data, *Geophys. Res. Lett.*, *29*(21), 2033, doi:10.1029/2001GL014480.

Moudry, D., H. Stenbaek-Nielsen, D. Sentman, and E. Wescott (2003), Imaging of elves, halos and sprite initiation at 1 ms time resolution, *J. Atmos. Sol.-Terr. Phys.*, *65*, 509–518.

Pasko, V. P., U. S. Inan, T. F. Bell, and Y. N. Taranenko (1997), Sprites produced by quasi-electrostatic heating and ionization in the lower ionosphere, *J. Geophys. Res.*, *102*, 4529–4561.

Pasko, V. P., M. A. Stanley, J. D. Mathews, U. S. Inan, and T. G. Wood (2002), Electrical discharge from a thundercloud top to the lower ionosphere, *Nature*, *416*, 152–154.

Rodger, C. J., M. Cho, M. A. Clilverd, and M. J. Rycroft (2001), Lower ionospheric modification by lightening-EMP: Simulation of the night ionosphere over the United States, *Geophys. Res. Lett.*, *28*, 199–202.

Sato, M., and H. Fukunishi (2003), Global sprite occurrence locations and rates derived from triangulation of transient Schumann resonance events, *Geophys. Res. Lett.*, *30*(16), 1859, doi:10.1029/2003GL017291.

Sentman, D. D., E. M. Wescott, D. L. Osborne, D. L. Hampton, and M. J. Heavner (1995), Preliminary results from the Sprites 94 aircraft campaign: 1. Red sprites, *Geophys. Res. Lett.*, *22*, 1205–1208.

Smith, D. A., X. Shao, D. Holden, C. Rhodes, M. Brook, P. Krehbiel, M. Stanley, W. Rison, and R. Thomas (1999), A distinct class of isolated intracloud lightning discharges and their associated radio emissions, *J. Geophys. Res.*, *104*, 4189–4212.

Su, H. T., R. R. Hsu, A. B. Chen, Y. J. Lee, and L. C. Lee (2002), Observation of sprites over the Asian continent and over oceans around Taiwan, *Geophys. Res. Lett.*, *29*(4), 1044, doi:10.1029/2001GL013737.

Su, H. T., et al. (2003), Gigantic jets between a thundercloud and the ionosphere, *Nature*, *423*, 974–976.

Takahashi, Y., et al. (2003), Activities of sprites and elves in the winter season, Japan, *J. Atmos. Terr. Phys.*, *65*, 551–560.

Thomas, J. N., et al. (2007), A very active sprite-producing storm observed over Argentina, *Eos Trans. AGU*, *88*(10), 117, doi:10.1029/2007EO100001.

Turman, B. N. (1977), Detection of lightning superbolts, *J. Geophys. Res.*, *82*, 2566–2568.

van der Velde, O. A., W. A. Lyons, T. E. Nelson, S. A. Cummer, J. Li, and J. Bunnell (2007), Analysis of the first gigantic jet recorded over continental North America, *J. Geophys. Res.*, *112*, D20104, doi:10.1029/2007JD008575.

Vazquez, J., K. Perry, and K. Kilpatrick (1998), NOAA/NASA AVHRR Oceans Pathfinder Sea Surface Temperature Data Set User's Reference Manual Version 4.0, JPL Publication D-14070.

Wacker, R. S., and R. E. Orville (1999), Changes in measured lightning flash count and return stroke peak current after the 1994 U.S. National Lightning Detection Network upgrade, *J. Geophys. Res.*, *104*, 2151–2157.

Wescott, E. M., D. D. Sentman, D. L. Osborne, D. L. Hampton, and M. J. Heavner (1995), Preliminary results from the Sprites 94 aircraft campaign: 2. Blue jets, *Geophys. Res. Lett.*, *22*, 1209–1212.

Williams, E., and N. Renno (1993), An analysis of the conditional instability of the tropical atmosphere, *Mon. Weather Rev.*, *121*, 21–36.

Yair, Y., et al. (2004), New observations of sprites from the space shuttle, *J. Geophys. Res.*, *109*, D15201, doi:10.1029/2003JD004497.

Y.-S. Chang and T.-Y. Liu, National Space Organization, 8F, 9 Prosperity 1st Road, HsinChu City, Hsinchu 30078, Taiwan.

A. B. Chen, R.-R. Hsu, C.-L. Kuo, Y.-J. Lee, and H.-T. Su, Department of Physics, National Cheng Kung University, 1 University Road, Tainan City, Tainan 70101, Taiwan. (htsu@phys.ncku.edu.tw)

J.-L. Chern, Department of Photonics, National Chiao Tung University, 1001 University Road, Hsinchu City, Hsinchu 30010, Taiwan.

H. U. Frey and S. B. Mende, Space Sciences Laboratory, University of California, 7 Gauss Way, Berkeley, CA 94720-7450, USA.

H. Fukunishi and Y. Takahashi, Department of Geophysics, Tohoku University, Aramaki, Aoba-ku, Miyagi 980-8578, Sendai, Japan.

L.-C. Lee, Institute of Space Science, National Central University, 300 Jhongda Road, Jhongli City, Taoyuan 32001, Taiwan.